The Class III POU Domain Protein Brn-1 Can Fully Replace the Related Oct-6 during Schwann Cell Development and Myelination

Ralf P. Friedrich,[1]† Beate Schlierf,[1]† Ernst R. Tamm,[2] Michael R. Bösl,[3]
and Michael Wegner[1]*

*Institut für Biochemie[1] and Institut für Anatomie,[2] Universität Erlangen-Nürnberg, Erlangen, and
Max-Planck-Institut für Neurobiologie, Martinsried,[3] Germany*

For differentiation, Schwann cells rely on the class III POU domain transcription factor Oct-6, which is expressed transiently when Schwann cells have established a one-to-one relation with axons but have not yet started to myelinate. Loss of Oct-6 leads to a transient arrest in this promyelinating stage and a delay in myelination. Although the closely related POU domain protein Brn-2 is coexpressed with Oct-6 in Schwann cells, its loss has only mild consequences. Combined loss of both POU domain proteins, in contrast, dramatically increases the myelination delay, raising the question of how related POU domain proteins compare to each other in their activities. Here, we have replaced Oct-6 expression in the mouse with expression of the class III POU domain protein Brn-1. Although this protein is not normally expressed in Schwann cells, Brn-1 was capable of fully replacing Oct-6. Brn-1 efficiently induced Krox-20 expression as a prerequisite for myelination. Onset and extent of myelination were also indistinguishable from that of the wild type in mice that carried only *Brn-1* instead of *Oct-6* alleles. Similar to Oct-6, Brn-1 down-regulated its own expression at later stages of myelination. Thus, class III POU domain proteins can fully replace each other in Schwann cell development.

Schwann cells are essential for development and function of peripheral nerves and have been studied extensively (24). Several signaling pathways influence proliferation, survival, commitment, and differentiation of Schwann cells (17). Cell-intrinsic regulators of Schwann cell development include transcription factors such as Pax-3 (9), c-Jun (33), Krox-20 (39), Sox10 (6, 19), and Oct-6 (25). These proteins show partially overlapping expression patterns and are needed during different stages of Schwann cell development (41, 42).

The POU domain protein Oct-6 (also known as SCIP or Tst-1) is induced in immature Schwann cells by an axonal signal shortly before 16.5 days postcoitum (dpc) (30). Expression reaches its peak in the consecutive promyelinating stage during early postnatal development, when Schwann cells have established a one-to-one relationship with axons and crucial changes in gene expression occur to prepare for myelination (2, 5, 22). In myelinating Schwann cells, Oct-6 is then gradually extinguished. Oct-6 functions at least partly through induction of Krox-20, the key activator of the myelination program (12).

Deletion of the *Oct-6* gene in mice led to an arrest of Schwann cell development at the promyelinating stage (4, 15). The transient nature of this arrest points to the existence of compensatory transcription factors in Schwann cells (10, 15). Compensatory mechanisms are frequently observed between closely related and functionally redundant transcription factors. Within the POU domain family, Oct-6 shows highest similarity to Brn-1, Brn-2, and Brn-4 (29, 43). These class III

POU domain proteins share similar biochemical properties (32).

Recent analyses have shown that Schwann cells express Brn-2 with the same developmental profile as Oct-6 (14). In agreement with functional redundancy between Oct-6 and Brn-2, combined deletion prolonged the arrest of Schwann cell differentiation, and transgenic expression of Brn-2 partially rescued the Schwann cell defect in Oct-6-deficient mice. However, functional redundancy was not complete, as only Oct-6-deficient mice and not Brn-2-deficient mice exhibited a Schwann cell phenotype. Additionally, a compensatory threefold increase of Brn-2 expression in Oct-6-deficient mice was unable to fully suppress the Schwann cell phenotype (14). It is unclear whether this incomplete functional redundancy results from differences in expression levels or from functional differences between class III POU domain proteins. Brn-1 is the class III POU domain protein with the most divergent DNA-binding and transactivation capacities in vitro (32). Differential functions of class III POU domain proteins might thus be most easily revealed by comparing the function of Oct-6 with that of Brn-1. For that reason, we replaced the *Oct-6* gene with the *Brn-1* gene and found that Schwann cell development in these knock-in mice proceeded on schedule.

MATERIALS AND METHODS

Construction of targeting vector. A 10.9-kb fragment from the *Oct-6* locus of 129/Sv mice (28) was used as the 5′ homology region. The open reading frame of rat *Brn-1* and the polyadenylation signal of the human growth hormone gene were inserted behind this 10.9-kb fragment so that the start codon of rat *Brn-1* was placed exactly over the start codon of *Oct-6*. A 4.6-kb fragment from the *Oct-6* locus containing the last 200 bp of the *Oct-6* open reading frame and 4.4 kb of downstream sequences (4) was used as the 3′ homology region. The combination of the 5′ homology region and rat *Brn-1* as well as the 3′ homology region were inserted into pTV-Flox-0 on either side of a *loxP*-flanked neomycin

* Corresponding author. Mailing address: Institut für Biochemie, Universität Erlangen, Fahrstrasse 17, 91054 Erlangen, Germany. Phone: 49-(0)9131-85-24620. Fax: 49-(0)9131-85-22484. E-mail: m.wegner @biochem.uni-erlangen.de.
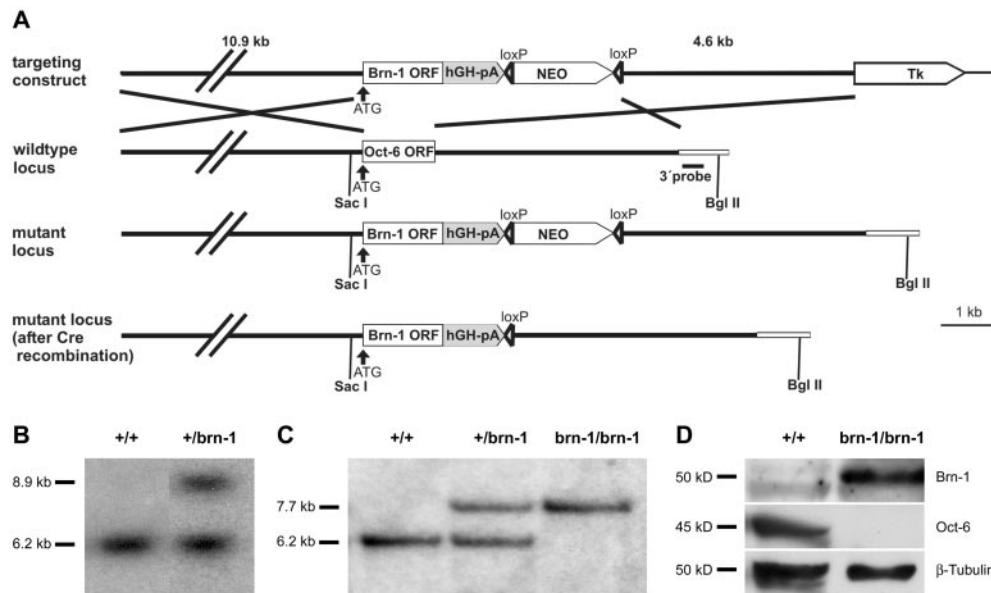† R.P.F. and B.S. contributed equally.

FIG. 1. Targeted replacement of *Oct-6* by *Brn-1* in mice. (A) Schematic representation, from top to bottom, of the targeting construct, the *Oct-6* wild-type locus, and the mutant locus before and after Cre recombination. The *Oct-6* and the *Brn-1* open reading frames (ORF) are shown as boxes, and 10.9- and 4.6-kb-long flanking regions are shown as bars. Regions of homology between the wild-type locus and targeting vector are depicted as black bars, and surrounding genomic regions not contained in the targeting construct are depicted as open bars. Plasmid backbone sequences of the targeting construct are indicated by a thin line. Restriction sites for SacI and BglII are shown as well as the localization of the 3′ probe and the start codon of the *Oct-6* gene (ATG). NEO, Neo cassette; hGH-pA, polyadenylation signal from the human growth hormone gene; loxP, recognition sites for Cre recombinase; Tk, herpes simplex virus thymidine kinase gene cassette. (B) Southern blot analysis of DNA from wild-type (+/+) and heterozygous (+/brn-1) ES cells digested with SacI and BglII for use of the 3′ probe. The size of bands corresponding to the wild type (6.2 kb) and the targeted allele (8.9 kb) are indicated. (C) Southern blot analysis of DNA from wild-type (+/+), Oct-6$^{+/Brn-1}$ (+/brn-1), and Oct-6$^{Brn-1/Brn-1}$ (brn-1/brn-1) mice digested with SacI and BglII for use of the 3′ probe after Cre-mediated removal of the Neo cassette. The sizes of bands corresponding to the wild type (6.2 kb) and the targeted allele (7.7 kb) are indicated. (D) Western blot of sciatic nerve extracts from 8-day-old wild-type (+/+) and Oct-6$^{Brn-1/Brn-1}$ (brn-1/brn-1) mice with antibodies directed against Brn-1, Oct-6, and β-tubulin. Molecular mass markers are indicated on the left.

resistance (Neo) cassette (Fig. 1A). The targeting vector thus replaced *Oct-6* with *Brn-1*. The construct was linearized with ClaI before electroporation.

Gene targeting and generation of mouse mutants. The linearized construct was electroporated into R1 ES cells (129 X1 × 129 S1) which were then selected with G418 (200 μg per ml) and ganciclovir (2 μM). Selected embryonic stem (ES) cell clones were screened by Southern blotting with a 0.3-kb 3′ probe which recognized a 6.2-kb fragment of the wild-type allele and an 8.9-kb fragment of the targeted allele in genomic DNA digested with SacI and BglII (Fig. 1A and B). Two targeted ES cell clones were injected into blastocysts to generate chimeras. Chimeric males from both clones transmitted the targeted allele to their offspring. No differences were detected between mice derived from the two ES cell clones. To remove the Neo cassette, heterozygous mutant mice were crossed with EIIa-Cre mice (20). In Southern blots on genomic DNA digested with SacI and BglII, loss of the Neo cassette resulted in a size reduction of the fragment indicative for the targeted allele from 8.9 to 7.7 kb (Fig. 1C).

Homozygous mutant mice were generated by intercrosses of Oct-6$^{+/Brn-1}$ animals. Alternatively, Oct-6$^{+/Brn-1}$ mice were crossed with Oct-6$^{+/lacZ}$ mice (4) to obtain Oct-6-deficient, mixed heterozygous Oct-6$^{Brn-1/lacZ}$ mice. Genotyping was routinely performed by PCR on genomic DNA obtained from tail tips or, in case of embryos, from yolk sacs. For the *Brn-1* knock-in allele, a common upper primer located 310 bp upstream of the start codon (5′-AGC CGG GCG GTG GTG GTG GG-3′) and two lower primers located 154 bp (5′-ACG TTC TGC ACT TCG CGG TAC GC-3′) and 28 bp (5′-GGT AGG GGT TAG AAG CCG CCG-3′) downstream of the start codon in *Oct-6* and *Brn-1*, respectively, were used. PCR was performed in 20-μl reaction mixtures containing standard buffer, 5% dimethyl sulfoxide, and 0.25 μM each primer. The cycling conditions consisted of an initial 3-min denaturing step at 94°C followed by 36 cycles of 30 s at 94°C, 30 s at 60°C, and 30 s at 72°C. A 470-bp fragment was indicative of the wild-type allele, and a 340-bp fragment was indicative of the targeted allele. Primers and PCR conditions for the *lacZ* knock-in allele have been described previously (4).

Western blotting. Isolated sciatic nerves were directly lysed in loading buffer, which was followed by sonication and heating in a boiling water bath. Samples were loaded onto denaturing sodium dodecyl sulfate–12.5% polyacrylamide gels and blotted onto nitrocellulose membranes (34). Polyclonal antisera directed against Brn-1 or Oct-6 (1:3,000 dilution) (21, 32) and a monoclonal antibody directed against β-tubulin (1:2,000 dilution; Sigma) served as primary antibodies, and horseradish peroxidase-coupled protein A served as a secondary detection reagent in Western blots using the ECL detection system (32).

Histological analyses. Sciatic nerves were isolated from perfused mice at various times up to 5 months after birth and placed overnight at 4°C in cacodylate-buffered fixative containing 2.5% paraformaldehyde, 2.5% glutaraldehyde, and 0.05% picric acid. After overnight washing in 0.1 M sodium cacodylate (pH 7.3), sciatic nerves were postfixed in cacodylate-buffered 1% osmium tetroxide for 2 h, dehydrated in an ascending ethanol series, and embedded in Epon resin. For light microscopy, semithin sections (1-μm thickness) were stained with *para*-phenylene diamine (8) and viewed with a Leica microscope. For electron microscopy, ultrathin sections (50-nm thickness) were stained with uranyl acetate and lead citrate and examined with a Zeiss EM902 electron microscope. Quantification of myelinating figures compared to promyelinating figures (300 to 600 fibers per nerve) was performed as described previously (14).

Immunohistochemistry. Embryos were obtained from staged pregnancies at 14.5 and 16.5 dpc, and sciatic nerves were obtained from postnatal mice at various ages. After fixation in 4% paraformaldehyde, specimens were cryoprotected by overnight incubation at 4°C in 30% sucrose and embedded in optimal cutting temperature medium at −80°C. Frozen sections were prepared at 10-μm thickness and used for immunohistochemistry as described previously (36, 37). The following primary antibodies were used in various combinations: anti-Sox10 guinea pig antiserum (1:2,000 dilution) (36), anti-Brn-1 guinea pig antiserum (1:1,000 dilution), anti-Oct-6 rabbit antiserum (1:1,500 dilution) (34), anti-Krox-20 rabbit antiserum (1:1,000 dilution) (35) anti-myelin basic protein (MBP) mouse monoclonal antibody (1:500 dilution; Chemicon), and anti-myelin protein

zero (MPZ) mouse monoclonal antibody (1:10,000 dilution; a gift of J. J. Archelos). Secondary antibodies conjugated to Cy2 and Cy3 immunofluorescent dyes (Dianova) were used for detection. Samples were analyzed and documented by using either a Leica TCS SL confocal microscope or a Leica inverted microscope (DMIRB) equipped with a cooled MicroMax charge-coupled-device camera (Princeton Instruments, Trenton, N.J.).

RESULTS

Replacement of the *Oct-6* gene with *Brn-1*. All class III POU domain proteins are coded for by intronless genes which are localized on different mouse chromosomes (3). To exchange *Oct-6* with *Brn-1*, we replaced the *Oct-6* open reading frame with the open reading frame of the rat *Brn-1* gene (32) and a Neo cassette. The start codon of *Brn-1* was placed exactly over the start codon of the *Oct-6* gene (Fig. 1A). To minimize alterations at the *Oct-6* gene locus, the Neo cassette was removed after germ line transmission of the targeted allele in the resulting heterozygous mice by Cre-mediated recombination (Fig. 1A and C). Oct-6$^{+/Brn-1}$ mice were viable and indistinguishable from their wild-type littermates on a gross anatomical and behavioral level. Western blot analysis confirmed that at postnatal day 8, Brn-1 was expressed in the myelinating sciatic nerve of mice carrying the *Brn-1* knock-in allele but not in those of wild-type littermates (Fig. 1D). Five weeks after birth, Brn-1 expression was no longer detectable in sciatic nerve extracts from mice carrying the knock-in allele (data not shown). Oct-6$^{+/Brn-1}$ mice were successfully intercrossed (Fig. 1C) and additionally bred with Oct-6$^{+/lacZ}$ mice (4) to obtain Oct-6$^{Brn-1/Brn-1}$ and Oct-6$^{lacZ/Brn-1}$ mice (Fig. 1C). Sciatic nerve extracts from these mice were devoid of Oct-6 protein at postnatal day 8 (Fig. 1D), thus corroborating the complete replacement of *Oct-6* with *Brn-1* in the knock-in allele.

Analysis of Brn-1 expression in peripheral nerves. Expression of Brn-1 from the knock-in allele was compared with that of the endogenous Oct-6 in the Schwann cell lineage by immunohistochemistry on Oct-6$^{+/Brn-1}$ embryos. Brn-1 protein was absent in peripheral nerves at 14.5 dpc (Fig. 2A), although Schwann cell precursors were already present along the nerve at this time, as evident from staining with Sox10-specific antibodies (Fig. 2E and F). Brn-1 became detectable at 16.5 dpc in nuclei of immature Schwann cells along the nerves of Oct-6$^{+/Brn-1}$ mice (Fig. 2B). Its spatiotemporal expression pattern strongly resembled that of the endogenous Oct-6 (Fig. 2C and D). In fact, coimmunohistochemistry performed on peripheral nerves of Oct-6$^{+/Brn-1}$ embryos at 16.5 dpc with antibodies directed against Oct-6 and Brn-1 yielded a perfect colocalization (Fig. 2, compare panels B and D).

We also analyzed expression of Brn-1 from the knock-in allele in the sciatic nerve through postnatal development. As previously described for Oct-6 (2, 15), and reproduced for Oct-6 on wild-type mice in this study (Fig. 3A, D, G, J, and M), the number of Brn-1-positive cells increased after birth in the nerve of Oct-6$^{+/Brn-1}$ mice (Fig. 3B and E), peaked during the first 2 postnatal weeks concomitant with the peak of myelination (Fig. 3H and K), and then gradually decreased. By postnatal day 56, Brn-1-positive cells were hardly detectable (Fig. 3O). Staining for Brn-1 and Oct-6 completely overlapped in Oct-6$^{+/Brn-1}$ mice (Fig. 3B, E, H, K, and N), thus arguing that expression of endogenous *Oct-6* and the *Brn-1* knock-in allele are qualitatively indistinguishable at all stages analyzed. Inter-
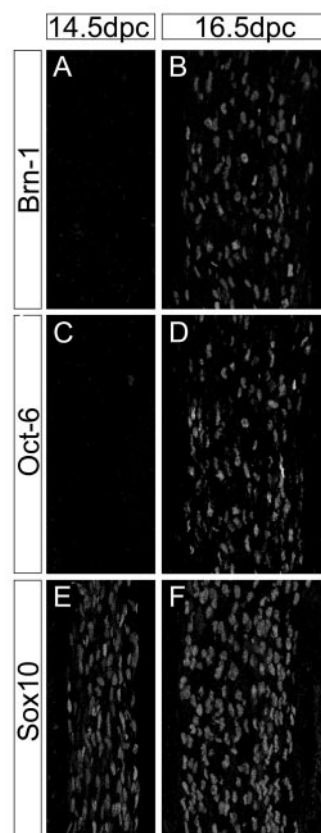

FIG. 2. Comparative expression of Oct-6 and Brn-1 in the peripheral nerve during embryonic development. Shown is an immunohistological analysis of peripheral nerves from Oct-6$^{+/Brn-1}$ embryos at 14.5 dpc (A, C, and E) and 16.5 dpc (B, D, and F) using antibodies against Brn-1 (A and B), Oct-6 (C and D), and Sox10 (E and F). Note that panels A and C as well as panels B and D were recorded from single sections following coimmunohistochemistry.

estingly, the same pattern of Brn-1 expression was observed in Oct-6$^{Brn-1/Brn-1}$ and Oct-6$^{Brn-1/lacZ}$ embryos, including a timely down-regulation in the absence of endogenous Oct-6 (Fig. 3C, F, I, L, and O and data not shown). Taking into account that Oct-6 has been shown to be involved in the down-regulation of its own expression (16), we thus have to assume that Brn-1 possesses the same capacity.

Expression of Krox-20 in mice carrying the *Brn-1* knock-in allele. As an early step in the activation of the myelination program, Oct-6 induces Krox-20 in promyelinating Schwann cells (12). Whether Brn-1 was capable of activating *Krox-20* gene expression in Schwann cells was analyzed by comparing occurrence and distribution of Krox-20 immunoreactivity in early postnatal sciatic nerves of wild-type mice (Fig. 4A and D) with those of Oct-6$^{Brn-1/Brn-1}$ (Fig. 4B and E) and Oct-6$^{Brn-1/lacZ}$ (Fig. 4C and F) mice. In all three genotypes, Krox-20 was present in the nuclei of a significant number of Schwann cells in the perinatal sciatic nerve (Fig. 4A to C). This number increased robustly during the following 4 days, independent of whether Oct-6 was present in the nerve or replaced by Brn-1 (Fig. 4D to F). Interestingly, Krox-20 induction remained unchanged even in Oct-6$^{Brn-1/lacZ}$ mice which express Brn-1 only
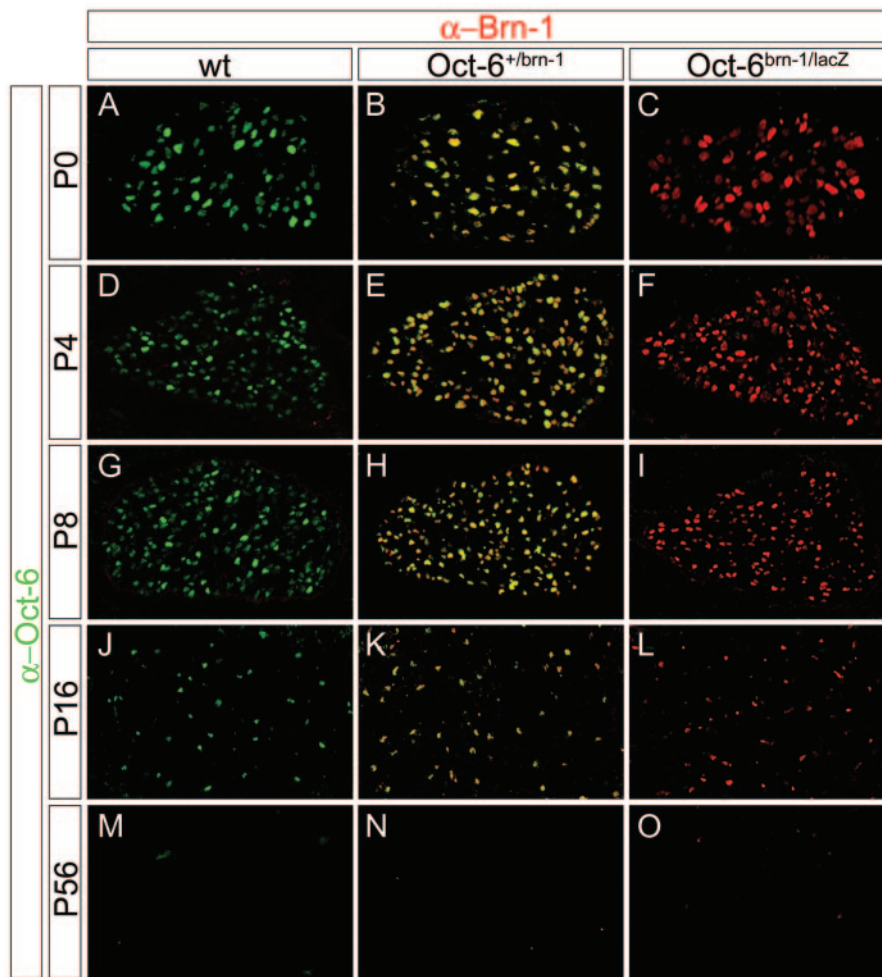
FIG. 3. Comparative expression of Oct-6 and Brn-1 in the postnatal sciatic nerve. Shown is coimmunohistochemistry on transverse sections of sciatic nerves (comparable levels) from wild-type (wt) (A, D, G, J, and M), Oct-6$^{+/Brn-1}$ (B, E, H, K, and N), and Oct-6$^{Brn-1/lacZ}$ (C, F, I, L, and O) mice at postnatal day 0 (P0) (A to C), day 4 (P4) (D to F), day 8 (P8) (G to I), day 16 (P16) (J to L), and day 56 (P56) (M to O) using antibodies against Oct-6 (α-Oct-6, green) in combination with antibodies against Brn-1 (α-Brn-1, red). Yellow color in sciatic nerves of Oct-6$^{+/Brn-1}$ mice indicates coexpression of both proteins.

from a single knock-in allele. Thus, Brn-1 mediates full Krox-20 induction even at half the normal gene dosage.

Expression of myelin proteins in mice carrying the *Brn-1* knock-in allele. Expression of myelin proteins was studied by immunohistochemistry to determine the onset and progression of myelination in the early postnatal sciatic nerve. In the wild type, MBP was present at detectable amounts in few Schwann cells of the sciatic nerve at the time of birth (Fig. 5A). Four days later, many MBP-expressing cells were already detected (Fig. 5D). Their number further increased through the first 2 weeks (Fig. 5G and J). At 5 weeks of age, the number of MBP-expressing Schwann cells had reached a constant level that was maintained throughout the remaining postnatal life (Fig. 5M and data not shown). MBP expression was similar in Oct-6$^{+/lacZ}$ mice with only a single functional *Oct-6* allele (data not shown), corroborating that *Oct-6* is haplosufficient for peripheral myelination (4, 15).

When studies were performed on sciatic nerves of Oct-6$^{Brn-1/Brn-1}$ pups, a comparable MBP expression profile

was obtained with few cells being detectable at the time of birth and a rapid increase of MBP-positive cells during the first 2 weeks (Fig. 5B, E, H, and K). MBP expression in the adult sciatic nerve of Oct-6$^{Brn-1/Brn-1}$ mice was also indistinguishable from that of the wild type (Fig. 5N). Again, MBP expression was unchanged even in Oct-6$^{Brn-1/lacZ}$ mice, arguing that even a single *Brn-1* knock-in allele is capable of maintaining normal levels and kinetics of MBP expression in the sciatic nerve (Fig. 5C, F, I, L, and O).

Expression in the sciatic nerve was also analyzed for the peripheral MPZ (Fig. 6). Neither visual inspection nor quantification revealed significant differences in the appearance or final number of MPZ-expressing cells in the sciatic nerve between genotypes. Both Oct-6$^{Brn-1/Brn-1}$ and Oct-6$^{Brn-1/lacZ}$ mice contained comparable numbers of MPZ-expressing cells at all times analyzed (Fig. 6, compare panels B, E, and H and C, F, and I to panels A, D, and G). Additionally, there were no obvious differences in staining intensities between the various genotypes even at early times (Fig. 6A to C). Thus, we found
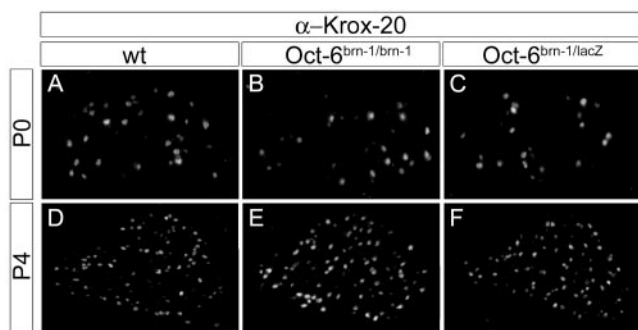
FIG. 4. Expression of Krox-20 in the postnatal sciatic nerve of mice carrying the *Brn-1* knock-in allele. Shown is an immunohistological analysis of sciatic nerves (comparable levels) from wild-type (wt) (A and D), Oct-6$^{Brn-1/Brn-1}$ (B and E), and Oct-6$^{Brn-1/lacZ}$ (C and F) mice at postnatal day 0 (P0) (A to C) and day 4 (P4) (D to F) using antibodies directed against Krox-20 (α-Krox-20).

no evidence of altered expression for two differentially and independently regulated myelin proteins in mice with the *Brn-1* knock-in allele. This result argues that expression of myelin proteins does not depend on the exact class III POU domain expressed in myelinating Schwann cells.

Myelination in mice carrying the *Brn-1* knock-in allele. As myelination can be disturbed in the presence of normal
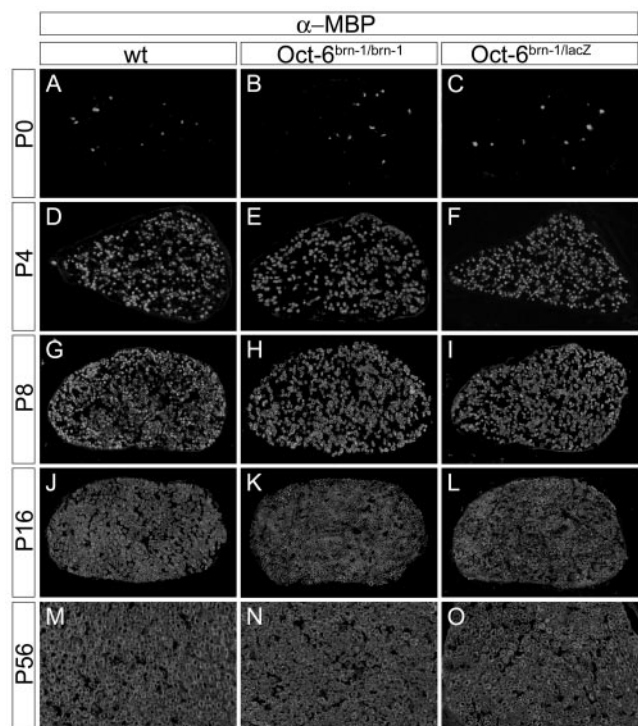

FIG. 5. Expression of MBP in the postnatal sciatic nerve of mice carrying the *Brn-1* knock-in allele. Shown is immunohistological analysis of transverse sections of sciatic nerves (comparable levels) from wild-type (wt) (A, D, G, J, and M), Oct-6$^{Brn-1/Brn-1}$ (B, E, H, K, and N), and Oct-6$^{Brn-1/lacZ}$ (C, F, I, L, and O) mice at postnatal day 0 (P0) (A to C), day 4 (P4) (D to F), day 8 (P8) (G to I), day 16 (P16) (J to L), and day 56 (P56) (M to O) using antibodies directed against myelin basic protein (α-MBP).
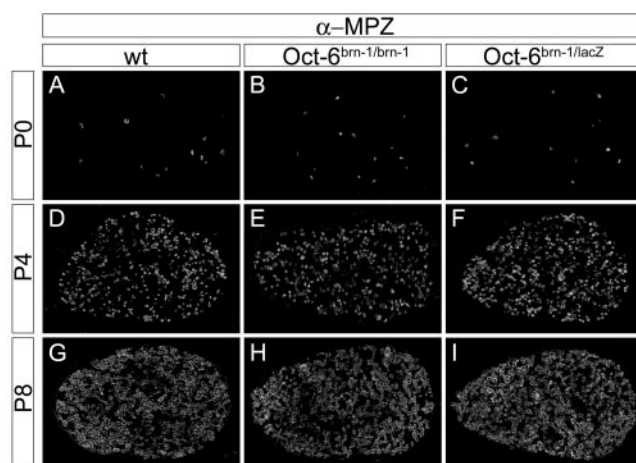

FIG. 6. Expression of protein zero in the postnatal sciatic nerve of mice carrying the *Brn-1* knock-in allele. Shown is immunohistological analysis of transverse sections of sciatic nerves (comparable levels) from wild-type (wt) (A, D, and G), Oct-6$^{Brn-1/Brn-1}$ (B, E, and H), and Oct-6$^{Brn-1/lacZ}$ (C, F, and I) mice at postnatal day 0 (P0) (A to C), day 4 (P4) (D to F), and day 8 (P8) (G to I) using antibodies directed against myelin protein zero (α-MPZ).

amounts of myelin proteins, formation and number of myelin sheaths were studied following *para*-phenylenediamine staining of Epon-embedded sciatic nerves. In agreement with our expression studies on myelin proteins, very few myelin figures were present in the sciatic nerve of Oct-6$^{lacZ/Brn-1}$ and Oct-6$^{Brn-1/Brn-1}$ mice at the day of birth (Fig. 7B and data not shown). However, the number was comparable to those detected in wild-type mice (Fig. 7A), again confirming that myelination in the peripheral nervous system starts on schedule in mice carrying one or two *Brn-1* knock-in alleles. Furthermore, the number of myelin figures increased comparably in all genotypes during the active phase of myelination (Fig. 7, compare panels C, E, G, and I with panels D, F, H, and J). For a detailed quantification, we counted the number of fibers which were already myelinated as well as the number of fibers still present in the promyelinating configuration at various days of postnatal development and determined their ratio as a measure of the progressing myelination and nerve maturation (Fig. 8). These analyses showed that the fraction of fibers which are already in the myelinated configuration increased from 3 to 4% at the day of birth to 56 to 59% at postnatal day 4 in sciatic nerves from Oct-6$^{lacZ/Brn-1}$ and Oct-6$^{Brn-1/Brn-1}$ mice. At postnatal day 8, approximately 90% of all large-caliber axons were myelinated, and myelination of the sciatic nerve was almost complete at postnatal day 16 in Oct-6$^{lacZ/Brn-1}$ and Oct-6$^{Brn-1/Brn-1}$ mice. Given the fact that we obtained comparable numbers for age-matched wild-type animals, we conclude that nerve maturation and myelination proceeded normally in mice carrying the *Brn-1* knock-in allele. Further supporting the absence of a phenotype in the peripheral nervous system, average numbers of myelin figures per defined area were indistinguishable in the adult sciatic nerve for Oct-6$^{lacZ/Brn-1}$ and Oct-6$^{Brn-1/Brn-1}$ mice and their wild-type littermates (Fig. 7K and L).

Myelin ultrastructure in mice carrying the *Brn-1* knock-in allele. Finally, we analyzed the myelin structure in sciatic nerves from 5-month-old Oct-6$^{lacZ/Brn-1}$ mice (Fig. 9). Our
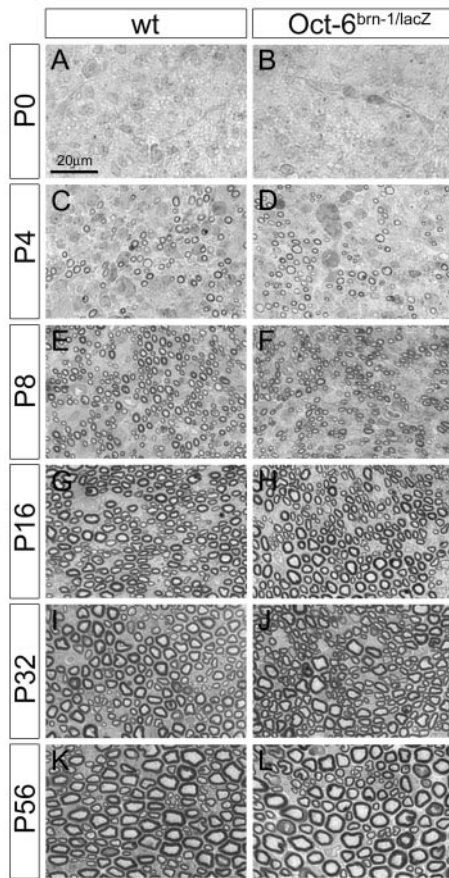
FIG. 7. Myelination in the postnatal sciatic nerve of mice carrying the *Brn-1* knock-in allele. Shown is *para*-phenylenediamine staining of myelin sheaths in transverse sections of sciatic nerves (comparable levels) from wild-type (wt) (A, C, E, G, I, and K) and Oct-6$^{Brn-1/lacZ}$ (B, D, F, H, J, and L) mice at postnatal day 0 (P0) (A and B), day 4 (P4) (C and D), day 8 (P8) (E and F), day 16 (P16) (G and H), day 32 (P32) (I and J), and day 56 (P56) (K and L).
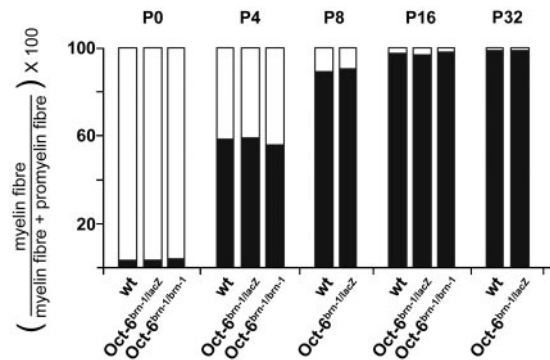

FIG. 8. Quantification of myelination in mice carrying the *Brn-1* knock-in allele. Myelin and promyelin fibers were quantified on transverse sciatic nerve sections from wild-type (wt), Oct-6$^{Brn-1/lacZ}$, and Oct-6$^{Brn-1/Brn-1}$ mice at day 0 (P0), day 4 (P4), day (P8), day 16 (P16), and day 32 (P32). Myelination was followed by determination of the relative contribution of myelin fibers to the sum of myelin and promyelin fibers.

cell development was transiently arrested at the promyelinating stage. The fact that this block was eventually overcome and myelination took place with delayed kinetics (10) hinted at the existence of a compensating activity within Schwann cells. This
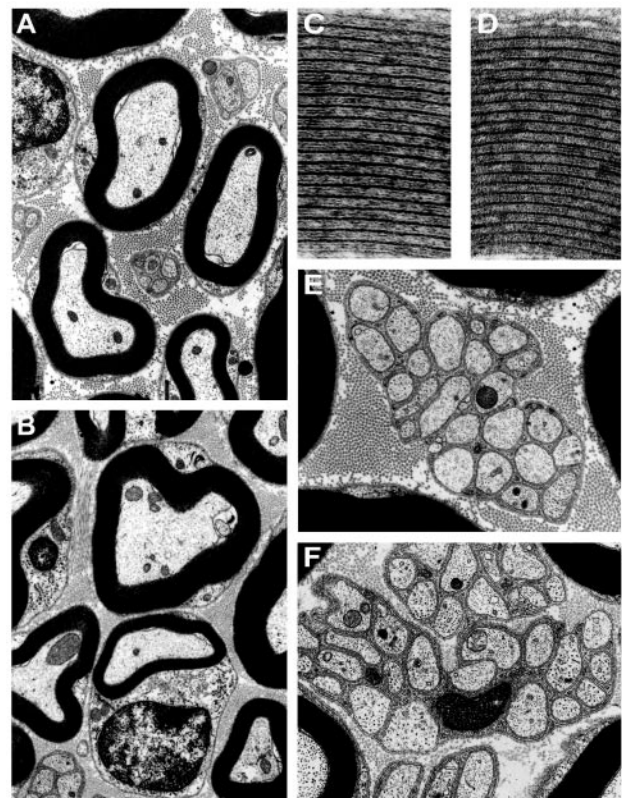
analysis revealed no conspicuous differences relative to age-matched wild-type samples. Both myelinating and nonmyelinating Schwann cells appeared normal in morphology (Fig. 9A, B, E, and F). Myelinating Schwann cells were in the typical 1:1 ratio with myelinated axons (Fig. 9A and B). Myelin sheaths exhibited a comparable thickness and a comparable number of turns for axons of comparable diameter in the wild type and the mutants (Fig. 9A to D). Compaction and membrane periodicity of the myelin sheath were equally normal in Oct-6$^{lacZ/Brn-1}$ mice (Fig. 9C and D). A basal lamina was always present (Fig. 9A and B). Up to 5 months of age, we found no myelin abnormalities, myelin debris, or signs of macrophage infiltration, arguing for a lack of nerve degeneration in Oct-6$^{lacZ/Brn-1}$ mice.

DISCUSSION

Over the last years, Oct-6 has been established as an important, cell-autonomous regulator of Schwann cell development which is primarily active at the promyelinating and early myelinating stage (2, 44) and required for normal progression through these stages (4, 15). In the absence of Oct-6, Schwann

FIG. 9. Myelin ultrastructure in mice carrying the *Brn-1* knock-in allele. Ultrathin sections from 5-month-old wild-type (A, C, and E) and Oct-6$^{Brn-1/lacZ}$ (B, D, and F) mice were recorded by electron microscopy to show myelinating (A and B) and nonmyelinating (E and F) Schwann cells and the periodicity of myelin sheaths from axons with comparable calibers (C and D). Magnifications, ×8,400 (A and B), ×168,000 (C and D), and ×14,400 (E and F).

activity was shown to be identical to Brn-2, a closely related class III POU domain protein coexpressed with Oct-6 in the Schwann cell lineage (14). In both gain-of-function and loss-of-function analyses, this compensation was only partial because of either different expression levels or functional differences between the two proteins. Although in vitro studies had previously failed to detect significant differences in DNA-binding or transactivation capacities between Oct-6 and Brn-2 (32), those studies might have missed differences imposed on the two proteins by the specific environment of the Schwann cell. Here, we have addressed the question of equivalency between class III POU domain proteins in vivo by replacing the *Oct-6* gene with the related *Brn-1*. Brn-1 was chosen over Brn-2 to maximize the chance of detecting functional differences. Brn-1 is evolutionarily less related to Oct-6 (13) and exhibited more biochemical differences from Oct-6 in vitro than Brn-2 (18, 19, 32). Furthermore, Brn-1 is not normally expressed in the Schwann cell lineage, so ectopic expression is easily detected. Finally, Brn-1 was chosen over the class III POU domain protein Brn-4 because it is coexpressed with Oct-6 and Brn-2 in oligodendrocytes, the counterparts of myelinating Schwann cells in the central nervous system (7, 32). Thus, our results with Brn-1 in Schwann cells might have predictive value for its relationship to other POU domain proteins and its function in oligodendrocytes.

During gene targeting, we did not remove any of the previously mapped hypersensitive sites in the vicinity of the *Oct-6* gene, including the Schwann cell-specific enhancer that was previously mapped 12 kb downstream of the open reading frame (22). Our knock-in resembles the previous replacement of *Oct-6* with a *lacZ* reporter (4). As the β-galactosidase expressed from this *lacZ* reporter faithfully recapitulated Oct-6 expression (2, 4), Brn-1 expression from this knock-in allele was expected to mimic the endogenous Oct-6 expression. Brn-1 expression started at the same time as endogenous Oct-6 expression, implying that it was dependent as much on axonal contact as Oct-6 expression (30). Furthermore, Brn-1 expression was extinguished in myelinating Schwann cells. It has previously been shown that Oct-6 is responsible for its own down-regulation in myelinating Schwann cells (16). As Brn-1 expression terminated with kinetics similar to that of Oct-6, even in Oct-6$^{Brn-1/Brn-1}$ animals, Brn-1 must be capable of down-regulating its own expression from the *Oct-6* locus.

Myelination in animals carrying the *Brn-1* knock-in allele was indistinguishable from that of wild-type mice. Previous results had shown that amounts of both MBP and MPZ were dramatically decreased in Oct-6-deficient Schwann cells throughout the first 2 weeks of postnatal development (4, 10, 15). In sciatic nerves of Oct-6$^{Brn-1/Brn-1}$ animals, however, both the number of annular structures positive for either MBP or MPZ as well as their staining intensity were normal. Oct-6 does not directly regulate expression of these myelin genes. Rather, Oct-6 activates Krox-20 expression (12), which in turn is responsible for the induction of myelin gene expression (26). Krox-20 expression was also normally activated by Brn-1 in Schwann cells.

As myelin gene expression is not the only criterion for myelination, we also studied formation and structure of myelin sheaths. Again, we failed to detect any significant abnormalities in animals carrying the *Brn-1* knock-in allele. Quantifica-

tion confirmed that the transformation of promyelinating figures to myelinating figures was completely on schedule in the postnatal sciatic nerve. Myelin sheath thickness and compaction was as normal as the basal lamina. Thus, Brn-1 is capable of efficiently driving Schwann cell myelination when expressed from the *Oct-6* locus.

Even more surprisingly, a single copy of the *Brn-1* knock-in allele on an otherwise *Oct-6*-deficient background (Oct-6$^{lacZ/Brn-1}$ animals) was sufficient to retain wild-type levels and kinetics of peripheral nerve myelination. Previous studies on a hypomorphic *Oct-6* allele had shown that once below 50% of wild-type levels, the amount of Oct-6 is rate limiting for myelination (10). Our results with Oct-6$^{lacZ/Brn-1}$ animals are therefore strongly indicative of a near-complete equivalency of Brn-1 and Oct-6 during Schwann cell development.

This finding has implications for the previously observed partial redundancy between Oct-6 and Brn-2 during Schwann cell development (14). We consider it more likely that different levels of expression are responsible for the different impact of both proteins on Schwann cell development rather than fundamentally different biological activities. We have previously proposed a similar model for the role of the related high-mobility-group domain transcription factors Sox8 and Sox10 during terminal differentiation of oligodendrocytes (36).

Our results might also be helpful in understanding the role of class III POU domains during oligodendrocyte development. Promyelinating oligodendrocytes express Oct-6, Brn-2, and Brn-1 (7, 32). If we assume that these proteins are functionally redundant in oligodendrocytes as well, it follows that the loss of each of these class III POU domain proteins is likely to be tolerated and compensated for by the remaining two proteins. Analyses of single knockouts for *Oct-6* and *Brn-2* support such an assumption (4, 15, 31). Furthermore, redundancy between class III POU domain proteins is not unheard of in the central nervous system and has been shown to exist between Brn-1 and Brn-2 during production, migration, and positioning of cortical neurons (23, 38).

Functional similarities between Oct-6 and Brn-1 per se might not be unexpected given the close relationship between these two proteins. A functional overlap had even been shown between Oct-6 and the much-less-related POU domain protein Skn-1 during differentiation of epidermal keratinocytes (1). However, given the fact that at least some POU domain proteins such as Brn-5 are completely unable to substitute for Oct-6 during Schwann cell development (14), the complete equivalency between Oct-6 and Brn-1 is surprising.

Previous studies have led to the hypothesis that a specific partner code for POU domain proteins and Sox proteins exists (18, 19), with Oct-6 being a partner for Sox10, which is also expressed in Schwann cells and essential for various phases of their development (6, 27). In contrast, Brn-1 appeared to be ineffective as a Sox10 partner (19). How can this differential cooperation with Sox10 be reconciled with the observed equivalency of Brn-1 and Oct-6 during Schwann cell development? In one explanation, cooperation with Sox10 is simply not essential for class III POU domain function during Schwann cell development. However, previous studies on the regulation of Krox-20 expression in Schwann cells are strongly suggestive of regulation by both Oct-6 and Sox10 (11).

Alternatively, Brn-1 might interact with a different Sox part-

ner protein such as Sox4, which is also present in Schwann cells at the right time (40). Closer attention might also be paid to the specific conditions in which cooperativity between POU domain proteins and Sox proteins was recorded. Originally, a composite element from the FGF-4 enhancer was studied in the U138 human astrocytoma cell line (18, 19). Thus, it is possible that the exact nature of the regulatory element as well as the cellular context contribute to the observed partner code. Even if Brn-1 and Sox10 did not cooperate on the FGF-4 enhancer element in Schwann cells, they might do so on Schwann cell-specific promoters. A final answer to this question will have to await the identification of Schwann cell-specific joint target genes for Oct-6 and Sox10 and the analyses of composite conditional mutants in which both Oct-6 and Sox10 are selectively deleted in promyelinating Schwann cells.

REFERENCES

1. **Andersen, B., W. C. Weinberg, O. Rennekampff, R. J. McEvilly, J. R. Bermingham, Jr., F. Hooshmand, V. Vasilyev, J. F. Hansbrough, M. R. Pittelkow, S. H. Yuspa, and M. G. Rosenfeld.** 1997. Functions of the POU domain genes Skn-1a/i and Tst-1/Oct-6/SCIP in epidermal differentiation. Genes Dev. **11:**1873–1884.
2. **Arroyo, E. J., J. R. Bermingham, M. G. Rosenfeld, and S. S. Scherer.** 1998. Promyelinating Schwann cells express Tst-1/SCIP/Oct-6. J. Neurosci. **18:** 7891–7902.
3. **Avraham, K. B., B. C. Cho, D. Gilbert, H. Fujii, K. Okamoto, T. Shimazaki, T. Ito, H. Shoji, Y. Wakamatsu, H. Kondoh, et al.** 1993. Murine chromosomal location of four class III POU transcription factors. Genomics **18:**131–133.
4. **Bermingham, J. R., S. S. Scherer, S. O'Connell, E. Arroyo, K. A. Kalla, F. L. Powell, and M. G. Rosenfeld.** 1996. Tst-1/Oct-6/SCIP regulates a unique step in peripheral myelination and is required for normal respiration. Genes Dev. **10:**1751–1762.
5. **Blanchard, A. D., A. Sinanan, E. Parmantier, R. Zwart, L. Broos, D. Meijer, C. Meier, K. R. Jessen, and R. Mirsky.** 1996. Oct-6 (SCIP/Tst-1) is expressed in Schwann cell precursors, embryonic Schwann cells, and postnatal myelinating Schwann cells: comparison with Oct-1, Krox-20, and Pax-3. J. Neurosci. Res. **46:**630–640.
6. **Britsch, S., D. E. Goerich, D. Riethmacher, R. I. Peirano, M. Rossner, K. A. Nave, C. Birchmeier, and M. Wegner.** 2001. The transcription factor Sox10 is a key regulator of peripheral glial development. Genes Dev. **15:**66–78.
7. **Collarini, E. J., R. Kuhn, C. J. Marshall, E. S. Monuki, G. Lemke, and W. D. Richardson.** 1992. Down-regulation of the POU transcription factor SCIP is an early event in oligodendrocyte differentiation in vitro. Development **116:** 193–200.
8. **Estable-Puig, J. F., W. C. Bauer, and J. M. Blumberg.** 1965. Technical note: paraphenylendiamine staining of osmium-fixed plastic embedded tissue for light and phase microscopy. J. Neuropathol. Exp. Neurol. **24:**531–536.
9. **Franz, T., and R. Kothary.** 1993. Characterization of the neural crest defect in Splotch (Sp^{1H}) mutant mice using a lacZ transgene. Dev. Brain Res. **72:**99–105.
10. **Ghazvini, M., W. Mandemakers, M. Jaegle, M. Piirsoo, S. Driegen, M. Koutsourakis, X. Smit, F. Grosveld, and D. Meijer.** 2002. A cell type-specific allele of the POU gene Oct-6 reveals Schwann cell autonomous function in nerve development and regeneration. EMBO J. **21:**4612–4620.
11. **Ghislain, J., C. Desmarquet-Trin-Dinh, P. Gilardi-Hebenstreit, P. Charnay, and M. Frain.** 2003. Neural crest patterning: autoregulatory and crest-specific elements co-operate for Krox20 transcriptional control. Development **130:**941–953.
12. **Ghislain, J., C. Desmarquet-Trin-Dinh, M. Jaegle, D. Meijer, P. Charnay, and M. Frain.** 2002. Characterisation of cis-acting sequences reveals a biphasic, axon-dependent regulation of Krox20 during Schwann cell development. Development **129:**155–166.
13. **Hara, Y., A. C. Rovescalli, Y. Kim, and M. Nirenberg.** 1992. Structure and evolution of four POU domain genes expressed in mouse brain. Proc. Natl. Acad. Sci. USA **89:**3280–3284.
14. **Jaegle, M., M. Ghazvini, W. Mandemakers, M. Piirsoo, S. Driegen, F. Levavasseur, S. Raghoenath, F. Grosveld, and D. Meijer.** 2003. The POU proteins Brn-2 and Oct-6 share important functions in Schwann cell development. Genes Dev. **17:**1380–1391.
15. **Jaegle, M., W. Mandemakers, L. Broos, R. Zwart, A. Karis, P. Visser, F. Grosveld, and D. Meijer.** 1996. The POU factor Oct-6 and Schwann cell differentiation. Science **273:**507–510.
16. **Jaegle, M., and D. Meijer.** 1998. Role of Oct-6 in Schwann cell differentiation. Microsc. Res. Tech. **41:**372–378.
17. **Jessen, K. R., and R. Mirsky.** 2002. Signals that determine Schwann cell identity. J. Anat. **200:**367–376.
18. **Kuhlbrodt, K., B. Herbarth, E. Sock, J. Enderich, I. Hermans-Borgmeyer, and M. Wegner.** 1998. Cooperative function of POU proteins and Sox proteins in glial cells. J. Biol. Chem. **273:**16050–16057.
19. **Kuhlbrodt, K., B. Herbarth, E. Sock, I. Hermans-Borgmeyer, and M. Wegner.** 1998. Sox10, a novel transcriptional modulator in glial cells. J. Neurosci. **18:**237–250.
20. **Lakso, M., J. G. Pichel, J. R. Gorman, B. Sauer, Y. Okamoto, E. Lee, F. W. Alt, and H. Westphal.** 1996. Efficient in vivo manipulation of mouse genomic sequences at the zygote stage. Proc. Natl. Acad. Sci. USA **93:**5860–5865.
21. **Leger, H., E. Sock, K. Renner, F. Grummt, and M. Wegner.** 1995. Functional interaction between the POU domain protein Tst-1/Oct-6 and the high-mobility-group protein HMG-I/Y. Mol. Cell. Biol. **15:**3738–3747.
22. **Mandemakers, W., R. Zwart, M. Jaegle, E. Walbeehm, P. Visser, F. Grosveld, and D. Meijer.** 2000. A distal Schwann cell-specific enhancer mediates axonal regulation of the Oct-6 transcription factor during peripheral nerve development and regeneration. EMBO J. **19:**2992–3003.
23. **McEvilly, R. J., M. O. de Diaz, M. D. Schonemann, F. Hooshmand, and M. G. Rosenfeld.** 2002. Transcriptional regulation of cortical neuron migration by POU domain factors. Science **295:**1528–1532.
24. **Mirsky, R., and K. R. Jessen.** 2001. Embryonic and postnatal development of Schwann cells, p. 1–20. In K. R. Jessen and W. D. Richardson (ed.), Glial cell development: basic principles and clinical relevance, 2nd ed. Oxford University Press, New York, N.Y.
25. **Monuki, E. S., G. Weinmaster, R. Kuhn, and G. Lemke.** 1989. SCIP: a glial POU domain gene regulated by cyclic AMP. Neuron **3:**783–793.
26. **Nagarajan, R., J. Svaren, N. Le, T. Araki, M. Watson, and J. Milbrandt.** 2001. EGR2 mutations in inherited neuropathies dominant-negatively inhibit myelin gene expression. Neuron **30:**355–368.
27. **Peirano, R. I., D. E. Goerich, D. Riethmacher, and M. Wegner.** 2000. Protein zero expression is regulated by the glial transcription factor Sox10. Mol. Cell. Biol. **20:**3198–3209.
28. **Renner, K., E. Sock, J. R. Bermingham, and M. Wegner.** 1996. Expression of the gene for the POU domain transcription factor Tst-1/Oct-6 is regulated by an estrogen-dependent enhancer. Nucleic Acids Res. **24:**4552–4557.
29. **Ryan, A. K., and M. G. Rosenfeld.** 1997. POU domain family values: flexibility, partnerships, and developmental codes. Genes Dev. **11:**1207–1225.
30. **Scherer, S. S., D. Wang, R. Kuhn, G. Lemke, L. Wrabetz, and J. Kamholz.** 1994. Axons regulate Schwann cell expression of the POU transcription factor SCIP. J. Neurosci. **14:**1930–1942.
31. **Schoneman, M. D., A. K. Ryan, R. J. McEvilly, S. M. O'Connell, C. A. Arias, K. A. Kalla, P. Li, P. E. Sawchenko, and M. G. Rosenfeld.** 1995. Development and survival of the endocrine hypothalamus and posterior pituitary gland requires the neuronal POU domain factor Brn-2. Genes Dev. **9:**3122–3135.
32. **Schreiber, J., J. Enderich, E. Sock, C. Schmidt, C. Richter-Landsberg, and M. Wegner.** 1997. Redundancy of class III POU proteins in the oligodendrocyte lineage. J. Biol. Chem. **272:**32286–32293.
33. **Shy, M. E., Y. Shi, L. Wrabetz, J. Kamholz, and S. S. Scherer.** 1996. Axon-Schwann cell interactions regulate the expression of c-jun in Schwann cells. J. Neurosci. Res. **43:**511–525.
34. **Sock, E., J. Enderich, M. G. Rosenfeld, and M. Wegner.** 1996. Identification of the nuclear localization signal of the POU domain protein Tst-1/Oct6. J. Biol. Chem. **271:**17512–17518.
35. **Sock, E., H. Leger, K. Kuhlbrodt, J. Schreiber, J. Enderich, C. Richter-Landsberg, and M. Wegner.** 1997. Expression of Krox proteins during differentiation of the O2-A progenitor cell line CG-4. J. Neurochem. **68:**1911–1919.
36. **Stolt, C. C., P. Lommes, R. P. Friedrich, and M. Wegner.** 2004. Transcription factors Sox8 and Sox10 perform non-equivalent roles during oligodendrocyte development despite functional redundancy. Development **131:**2349–2358.
37. **Stolt, C. C., P. Lommes, E. Sock, M.-C. Chaboissier, A. Schedl, and M. Wegner.** 2003. The Sox9 transcription factor determines glial fate choice in the developing spinal cord. Genes Dev. **17:**1677–1689.
38. **Sugitani, Y., S. Nakai, O. Minowa, M. Nishi, K. Jishage, H. Kawano, K. Mori, M. Ogawa, and T. Noda.** 2002. Brn-1 and Brn-2 share crucial roles in the production and positioning of mouse neocortical neurons. Genes Dev. **16:**1760–1765.
39. **Topilko, P., M. S. Schneider, G. Levi, V. E. A. Baron, A. B. Chennoufi, T. Seitanidou, C. Babinet, and P. Charnay.** 1994. Krox-20 controls myelination in the peripheral nervous system. Nature **371:**796–799.

40. **Verheijen, M. H., R. Chrast, P. Burrola, and G. Lemke.** 2003. Local regulation of fat metabolism in peripheral nerves. Genes Dev. **17:**2450–2464.

41. **Wegner, M.** 2000. Transcriptional control in myelinating glia: flavors and spices. Glia **31:**1–14.

42. **Wegner, M.** 2000. Transcriptional control in myelinating glia: the basic recipe. Glia **29:**118–123.

43. **Wegner, M., D. W. Drolet, and M. G. Rosenfeld.** 1993. POU-domain proteins: structure and function of developmental regulators. Curr. Opin. Cell Biol. **5:**488–498.

44. **Zorick, T. S., D. E. Syroid, E. Arroyo, S. S. Scherer, and G. Lemke.** 1996. The transcription factors SCIP and Krox-20 mark distinct stages and cell fates in Schwann cell differentiation. Mol. Cell. Neurosci. **8:**129–145.